

Highly Porous and Stable Metal–Organic Frameworks: Structure Design and Sorption Properties

Mohamed Eddaoudi,[†] Hailian Li,[‡] and O. M. Yaghi^{*,†}

Contribution from the Materials Design and Discovery Group, Department of Chemistry, University of Michigan, Ann Arbor, Michigan 48109-1055, and Department of Chemistry and Biochemistry, Arizona State University, Tempe, Arizona 85287-1604

Received September 14, 1999

Abstract: Gas sorption isotherm measurements performed on the evacuated derivatives of four porous metal–organic frameworks (MOF-*n*), Zn(BDC)·(DMF)(H₂O) (DMF = *N,N'*-dimethylformamide, BDC = 1,4-benzenedicarboxylate) (MOF-2), Zn₃(BDC)₃·6CH₃OH (MOF-3), Zn₂(BTC)NO₃·(C₂H₅OH)₅H₂O (BTC = 1,3,5-benzenetricarboxylate) (MOF-4), and Zn₄O(BDC)₃·(DMF)₈C₆H₅Cl (MOF-5), reveal type I isotherms for *n* = 2, 3, and 5, which is evidence of microporous and accessible channels having high structural integrity and organization. Although gas sorption into MOF-4 was not observed, careful examination of its ethanol sorption isotherms at 22 and 32 °C point to the presence of coordinatively unsaturated zinc centers within its pores, which upon ethanol sorption undergo coordination transitions from 3- to 4-, 4- to 5-, and 5- to 6-coordination. MOF-*n* materials were produced by building the extended analogues of molecular metal carboxylate clusters—a strategy that has allowed the realization of the most porous and thermally stable framework yet reported: the evacuated form of MOF-5 is especially stable in air at 300 °C and has a free pore volume representing 55–60% of its crystal as determined by gas sorption and single-crystal diffraction studies.

Introduction

Werner complexes, β-M(4-Methylpyridyl)₄(NCS)₂ (M = Ni²⁺ or Co²⁺),¹ Prussian blue compounds, Fe₄[Fe(CN)₆]₃·xH₂O (x = 14–16),² and Hofmann clathrates and their derivatives, Cd-(NH₃)₂Ni(CN)₄·G (G = guests such as C₆H₆ and C₁₂H₁₀),^{2c,3} are widely known as materials that can reversibly sorb small molecules. Open frameworks are also known to exist in numerous other coordination compounds such as copper(I) bis-(adiponitrilo) nitrate and Cu₃(en)₂(CN)₄·H₂O (en = ethylenediamine), however, their sorption behavior was not reported.⁴ Nevertheless, these compounds have inspired the current interest in the copolymerization of a wide range of larger organic linkers with metal-ions to yield new classes of designed metal–organic frameworks (MOF) having unusual open architecture and unprecedented pore size and shape.⁵ However, these frameworks are commonly plagued by their inability to support porosity: the removal of guests, incorporated during synthesis, or their exchange leads to collapse and decomposition of the framework, thus precluding study of their inclusion chemistry—an aspect that is critically important for their utility as porous materials.

Secondary Building Units (SBUs). Our approach to the preparation of robust frameworks has been to employ bis- and

tris-bidentate carboxylate linkers such as 1,4-benzenedicarboxylate (BDC) and 1,3,5-benzenetricarboxylate (BTC), which offer important advantages due to their rigidity and consequent tendency to form rigid metal carboxylate clusters that ultimately act as secondary building units (SBUs) in the extended solid. In fact, the extended structure analogues of molecular dinuclear, trinuclear, and tetranuclear zinc(II) carboxylate clusters (Figure 1)^{6a–d} have been successfully prepared using BDC and BTC as linkers to give Zn(BDC)·(DMF)(H₂O) (DMF = *N,N'*-dimethylformamide) (MOF-2), Zn₃(BDC)₃·6CH₃OH (MOF-3), Zn₂(BTC)(NO₃)·(C₂H₅OH)₅(H₂O) (MOF-4), and Zn₄O(BDC)₃·(DMF)₈(C₆H₅Cl) (MOF-5). The syntheses and atomic structures of these crystals have been reported and discussed in preliminary accounts.^{6e–h} The main focus of this report is to demonstrate, using sorption measurements, that such metal–organic frameworks can support permanent porosity and exhibit inclusion properties uncommon to traditional inorganic porous materials.

(5) For example: (a) *Structural Aspects of Inclusion Compounds Formed by Inorganic and Organometallic Host Lattices*; Atwood, J. T., Davies, J. E. D., MacNicol, D. D., Eds; Academic Press: London, 1984; Vol. 1. (b) Kitagawa, S.; Kondo, M. *Bull. Chem. Soc. Jpn.* **1998**, *71*, 1739. (c) Batten, S. R.; Robson, R. *Angew. Chem., Int. Ed.* **1998**, *37*, 1460. (d) Yaghi, O. M.; Li, H.; Davis, C.; Richardson, D.; Groy, T. L. *Acc. Chem. Res.* **1998**, *31*, 474. (e) Losier, P.; Zaworotko, M. J. *Angew. Chem., Int. Ed. Engl.* **1996**, *35*, 5, 2779. (f) Gardner, G. B.; Venkataraman, D.; Moore, J. S.; Lee, S. *Nature* **1995**, *374*, 792.

(6) Molecular Clusters: (a) Clegg, W.; Little, I. R.; Straughan, B. P. *J. Chem. Soc., Dalton Trans.* **1986**, 1283. (b) Clegg, W.; Little, I. R.; Straughan, B. P. *J. Chem. Soc., Chem. Commun.* **1985**, 73. (c) Clegg, W.; Harbron, D. R.; Homan, C. D.; Hunt, P. A.; Little, I. R.; Straughan, B. P. *Inorg. Chim. Acta* **1991**, *186*, 51. (d) Malik, M. A.; Motevallii, M.; O'Brien, P. *Inorg. Chem.* **1995**, *34*, 6223. Extended Analogues: (e) Li, H.; Eddaoudi, M.; Groy, T. L.; Yaghi, O. M. *J. Am. Chem. Soc.* **1998**, *120*, 8571. (f) Li, H.; Davis, C. E.; Groy, T. L.; Kelley, D. G.; Yaghi, O. M. *J. Am. Chem. Soc.* **1998**, *120*, 2186. (g) Yaghi, O. M.; Davis, C. E.; Li, G.; Li, H. *J. Am. Chem. Soc.* **1997**, *119*, 2861. (h) Li, H.; Eddaoudi, M.; O'Keeffe, M.; Yaghi, O. M. *Nature* **1999**, *402*, 276.

[†] University of Michigan.

[‡] Arizona State University.

(1) Barrer, R. M. In *Molecular Sieves*; Meier, W. M., Utyyehoeven, J. B., Eds.; ACS Advances in Chemistry Series 121; American Chemical Society: Washington, DC, 1974; p 1.

(2) Wilde, R. E.; Ghosh, S. N.; Marshall, B. *J. Inorg. Chem.* **1970**, *9*, 2512. (b) Buser, H. J.; Schwarzenbach, D.; Petter, W.; Ludi, A. *Inorg. Chem.* **1977**, *16*, 2704. (c) Dunbar, K. R.; Heintz, R. A. *Prog. Inorg. Chem.* **1997**, *45*, 283, and references therein.

(3) Iwamoto, T.; Miyoshi, T.; Sasaki, Y. *Acta Crystallogr.* **1974**, *B30*, 292.

(4) Kinoshita, Y.; Matsubara, I.; Higuchi, T.; Saito, Y. *Bull. Chem. Soc. Jpn.* **1959**, *32*, 1222. (b) Williams, R. J.; Larson, A. C.; Cromer, D. T. *Acta Crystallogr.* **1973**, *B28*, 858.

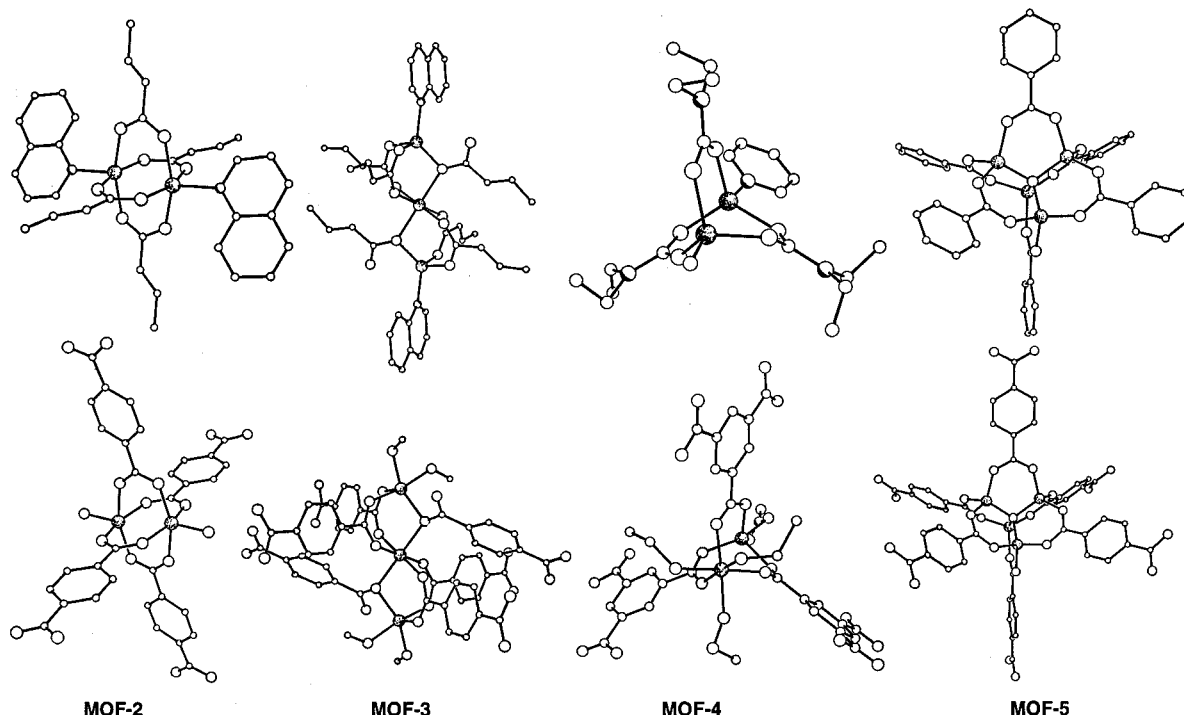


Figure 1. Summary of the structural relationship of the Zn–O–C cluster SBUs between discrete metal carboxylate clusters [top row: from left, $Zn_2(\text{crotonate})_4(\text{quinoline})_2$, $Zn_3(\text{crotonate})_6(\text{quinoline})_2$, $Zn_2(\text{CH}_3)(\text{carbamato})_3(\text{pyridine})$, and $Zn_4(\text{O})(\text{benzoate})_6$] and their extended analogues (MOF-2–5), respectively. Atoms are shown as spheres with Zn, shaded; O, large open; N, partially shaded; C, small open. Hydrogen atoms have been omitted for clarity.

Experimental Section

As-Synthesized Compounds. Crystalline samples of the as-synthesized form of the compounds MOF-2–5 were obtained using already published procedures. Their identity was confirmed using elemental microanalysis, thermal gravimetric analysis, FT-IR, X-ray single crystal studies, and X-ray powder diffraction (XRPD).^{6e–h}

Gas Sorption Isotherms. Sorption isotherm studies for all materials were performed by measuring the increase in weight at equilibrium as a function of relative pressure. Measurements were performed using a CAHN 1000 electrogravimetric balance using 1 mg scale (sensitivity 1 μg). A known weight (typically 100–150 mg) of the as-synthesized starting material was placed in a cylindrical quartz bucket (height = 30 mm, and o.d. \times i.d. = 19 \times 17 mm), then subjected to a heating program at pressures below 1×10^{-5} Torr in order to remove the guests and produce the evacuated form (vide infra). Pressures were measured with two MKS Baratron transducers 622A with the range covering 0–10 and 0–1000 Torr (accuracy 0.25%). The adsorbate was added incrementally. A point isotherm was recorded at equilibrium (the stage when no further weight change was observed and when the pressure changes were less than 1 mm-Torr/min.).

The N_2 , Ar, and CO_2 adsorbates were of UHP grade. The temperature of each sample was controlled by refrigerated bath of liquid nitrogen (-195°C) for N_2 and Ar, and dry ice/acetone (-78°C) for CO_2 . All organic solvents were anhydrous GC grade 99.8%, purchased from Aldrich Chemical Co. and stored over 3 \AA molecular sieves.

In the case of MOF-4, ethanol vapor uptake at constant pressure was described by a phenomenological model that is equivalent to a linear driving force model ($M_t/M_e = 1 - e^{-kt}$; M_t , gas uptake at time t ; M_e , gas uptake at equilibrium; k , rate constant).⁷

The nitrogen apparent Langmuir surface area was estimated using the Langmuir equation and assuming a monolayer coverage of N_2 using a cross-sectional area of 16.2 $\text{\AA}^2/\text{molecule}$. The pore volume was calculated by extrapolation of the Dubinin–Radushkevich equation, assuming the sorbate is in the liquid state and the sorption involves a pore-filling process.⁸

Liquid Sorption. Inclusion of guests from solution was studied by employing chromatographic (GC) techniques and using a Shimadzu CR 501 Chromtopac gas chromatograph having a $1/8'' \times 6'$ packed Alltech Carbograph NKA column at 150°C under He flow rate of 20 cm^3/min . A thermal conductivity detector was used in conjunction with an electronic strip chart recorder, which provided peak integrations for each sample.

In the solution isotherm experiments, solutions of known concentrations were prepared by mixing a known amount of potential guest molecule in toluene (2.00 mL). To this mixture, a known amount of the evacuated material (0.030 or 0.040 g) was added to yield a heterogeneous mixture. Immediate GC analysis of the supernatant revealed changes in the concentration of guests relative to that observed prior to the addition of the host solid. The association equilibrium constant for a specific guest was derived from the concentration range 0.10–1.00 M in toluene solution. The amount sorbed was measured as a function of guest equilibrium concentration, which was recorded at the point when no additional change in concentration was observed (~ 3 h). The experimental data was successfully fitted by nonlinear regression assuming a 1:1 stoichiometry of guest to binding sites. Generally, correlation coefficients of 0.999 were achieved.

Pore Dimensions. The pore cross-section was calculated by considering overlapping spheres with van der Waals radii using 1.5, 1.2, 1.7, and 1.5 \AA for Zn, H, C, and O, respectively.

Preparation of Evacuated Frameworks. All materials were evacuated in the CAHN sorption gravimetric apparatus under a pressure of 1×10^{-5} Torr and an appropriate heating program as outlined below. Measurement of constant weight with residual pressure of 1×10^{-5} Torr was recorded and interpreted as the points at which a discrete weight loss has been completed. Table 1 compares the elemental microanalysis of the evacuated products and those of the as-synthesized materials. The pore volume and nitrogen apparent surface area were calculated from the gas sorption isotherms for the evacuated frameworks as summarized in Table 2.

(8) (a) According to IUPAC classification: Sing, K. S. W.; Everett, D. H.; Haul, R. A. W.; Moscou, L.; Pierotti, R. A.; Rouquerol, J.; Siemieniowski, T. *Pure and Appl. Chem.* **1985**, *57*, 603–619. (b) Gregg, S. J.; Sing, K. S. W. *Adsorption, Surface Area, Porosity*, 2nd ed.; Academic Press: London, U.K., 1982.

(7) Foley, N. J.; Thomas, K. M.; Forshaw, P. L.; Stanton, F. D.; Norman, P. R. *Langmuir* **1997**, *13*, 2083.

Table 1. Calculated and Found Elemental Composition of As-Synthesized (A) and Evacuated (B) MOF-*n* (*n* = 2–5)

MOF- <i>n</i>	A				B			
	C	H	N	Zn	C	H	N	Zn
MOF-2	Zn(BDC)·(DMF)H ₂ O				Zn(BDC)			
	41.21	4.09	4.37	20.39	41.87	1.76	0.00	
	41.04	4.18	4.52	20.33	40.47	1.82	0.16	
MOF-3	Zn ₃ (BDC) ₃ ·(CH ₃ OH) ₆				Zn ₃ (BDC) ₃ ·(CH ₃ OH) ₂			
	40.91	4.12	0.00	22.27	41.49	2.68	0.00	26.06
	40.62	4.08	0.02	21.94	41.55	2.54	0.09	26.10
MOF-4	Zn ₂ (BTC)NO ₃ ·(C ₂ H ₅ OH) ₅ H ₂ O				Zn ₂ (BTC)(NO ₃)·C ₂ H ₅ OH			
	35.20	5.44	2.16	20.17	29.04	2.22	3.08	
	35.30	5.54	2.06	19.77	29.34	2.65	2.96	
MOF-5	Zn ₄ O(BDC) ₃ ·(DMF) ₈ C ₆ H ₅ Cl				Zn ₄ O(BDC) ₃			
	44.21	5.02	7.64	17.82	37.45	1.57	0.00	
	43.25	5.29	7.56	17.04	36.94	1.66	0.26	

Table 2. Sorption Capacity for MOF-*n* (*n* = 2–5)

MOF- <i>n</i>	guest	guest/ formula unit	guest/ unit cell	pore cross section (Å)	apparent surface area (m ² /g)	pore volume (cm ³ /g)
MOF-2	N ₂	0.63	2.52		270	0.094
	CO ₂	0.70	2.80			0.086
	CH ₂ Cl ₂	0.82	3.28	7		0.229
	CHCl ₃	0.64	2.56			0.222
	C ₆ H ₆	0.56	2.24			0.220
	C ₆ H ₁₂	0.47	1.88			0.221
MOF-3	N ₂	0.74	0.74		140	0.038
	Ar	0.71	0.71			0.036
	CO ₂	0.95	0.95			0.038
	CH ₂ Cl ₂	0.69	0.69			0.065
	CHCl ₃	0.56	0.56	8		0.065
	CCl ₄	0.45	0.45			0.065
MOF-4	C ₆ H ₆	0.50	0.50			0.064
	C ₆ H ₁₂	0.41	0.41			0.065
MOF-4	C ₂ H ₅ OH	4.60	18	14		0.612
MOF-5	N ₂	22.87	183		2900	1.04
	Ar	28.75	230			1.03
	CH ₂ Cl ₂	11.00	88	12		0.93
	CHCl ₃	8.86	71			0.94
	CCl ₄	7.38	59			0.94
	C ₆ H ₆	7.88	63			0.94
	C ₆ H ₁₂	6.38	51			0.92

Zn(BDC)·(DMF)(H₂O) (MOF-2) → Zn(BDC). MOF-2 (119.0 mg) was evacuated at room-temperature for 36 h, and the weight was found to be 109.9 mg (92.4%). Upon heating this sample to 140 °C for 16 h an additional weight loss of 20.63% was observed as summarized in Figure 2a. Sorption studies performed on the evacuated material are presented in Figure 2b–d. We have observed that this material reacts irreversibly with water to yield a nonporous phase.

Zn₃(BDC)₃·6CH₃OH (MOF-3) → Zn₃(BDC)₃. MOF-3 (64.98 mg) was found to lose weight readily at room-temperature under vacuum: a weight of 55.60 mg (85.56%) was recorded after 18 h as shown in Figure 3a. Upon heating to 140 °C, a steady weight loss was observed until the sample weight reached 50.91 mg (78.35%). The solution and gas sorption isotherms are shown in Figure 3b–d.

Zn₂(BTC)(NO₃)·(C₂H₅OH)₅(H₂O) (MOF-4) → Zn₂(BTC)(NO₃). MOF-4 (158.83 mg) was placed under vacuum at room-temperature for 48 h. The weight recorded at this point was 109.58 mg (68.80%) as shown in Figure 4a, however, after heating the sample to 72 °C for 16 h the weight measured was 98.90 mg (62.27%). The solution and gas sorption data are shown in Figure 4b–d.

Zn₄O(BDC)₃·(DMF)₈(C₆H₅Cl) (MOF-5) → Zn₄O(BDC)₃. Freshly prepared crystals of MOF-5 (150 mg) were washed with chloroform (6 × 30 mL) and immersed in chloroform (50 mL) for 18 h, then removed and immersed in a fresh chloroform solution for 1 h. The crystals were dried until no liquid chloroform on their surface was observed. The sample was placed under vacuum at room temperature

for 24 h to give a weight of 53.90 mg (54.55%). No additional weight loss was observed upon heating this sample to 110 °C for 12 h.

Results and Discussion

At the outset of this study, the sorption isotherms for metal–organic frameworks were largely unexplored with only few reports published.^{6e,9} This section presents the sorption isotherm behavior of MOF-2–5, and shows that these materials offer unusual inclusion chemistry. We show how coordination chemistry of metal ions can be exploited to allow for: the transformation of 2-D structures to 3-D porous frameworks (MOF-2), functionalization of the pore structure (MOF-3 and 4), and the formation of the most robust metal–organic framework yet observed (MOF-5).

Evacuated Frameworks. We have reported the XRPD for the as-synthesized and evacuated materials, which remain similar for a given MOF, thus indicating retention of the framework structure in the absence of guests.^{6e–h} Elemental analysis (Table 1) along with the thermal gravimetric analysis confirm the absence of guests and the formulation of the evacuated frameworks.

From 4⁴ Tiling Structure to 3-D Porous Framework. The Zn₂ dinuclear SBU in MOF-2 are polymerized by BDC to yield square sheets with a 4⁴ regular tiling topology (Figure 1).^{6e} DMF guest molecules occupy the square pores within the sheets, and one water ligand occupies the axial position on each Zn atom. In the crystal, water ligands separate the sheets which otherwise stack in registry to create 1-D channels with 7 Å cross-section. Heating the as-synthesized material results in two discrete weight loss steps at 7.6 and 20.63%, which together correspond to the loss of exactly one water and one DMF (calcd, 28.23%) per formula unit.

We have examined the bonding motif adopted between the layers and found that each zinc atom is ideally positioned from a nearby BDC oxygen of an adjacent layer, in that the Zn···O–C angle is 117.6 (7)°. Thus in the absence of water, the formation of stronger Zn···O interactions between the layers is likely as it does not require distortion or alteration of the stacking motif. We believe this leads to a stable 3-D porous Zn(BDC) framework.

Indeed, the N₂ and CO₂ gas sorption isotherms for Zn(BDC) showed reversible type I behavior (Figure 2b) characterized by a plateau reached at low relative pressure, which is indicative of sorption in micropores. A similar reversible uptake of organic solvents, chloroform, methylene chloride and benzene by this material was also observed as shown in Figure 2c. However, slight irregularities in the sorption behavior are apparent in the low-pressure region. These are magnified in the case of cyclohexane (Figure 2d): it appears to follow a more complex mechanism showing little sorption at the outset, followed by larger uptake and terminating with a plateau near the saturation region. This behavior along with the observed low-pressure hysteresis might be associated with distortion of the host structure to accommodate the guest, a process which is difficult to reverse in the case of cyclohexane. This observation is supported by the absence of such extreme sorption behavior for guests with smaller kinetic diameter (compare cyclohexane, 6.20 Å to chloroform, 4.60, methylene chloride, 4.00, and benzene, 5.85 Å). Thus, it is unclear whether the framework remains intact after cyclohexane removal.

(9) Allison, S. A.; Barrer, R. M. *J. Chem. Soc. (A)* **1969**, 1717–1723. (b) Ramprasad, D.; Pez, G. P.; Toby, B. H.; Markley, T. J.; Pearlstein, R. M. *J. Am. Chem. Soc.* **1995**, *117*, 10694–10701. (c) Kondo, M.; Yoshitomi, T.; Seki, K.; Matsuzaka, H.; Kitagawa, S. *Angew. Chem., Int. Ed. Engl.* **1997**, *36*, 1725.

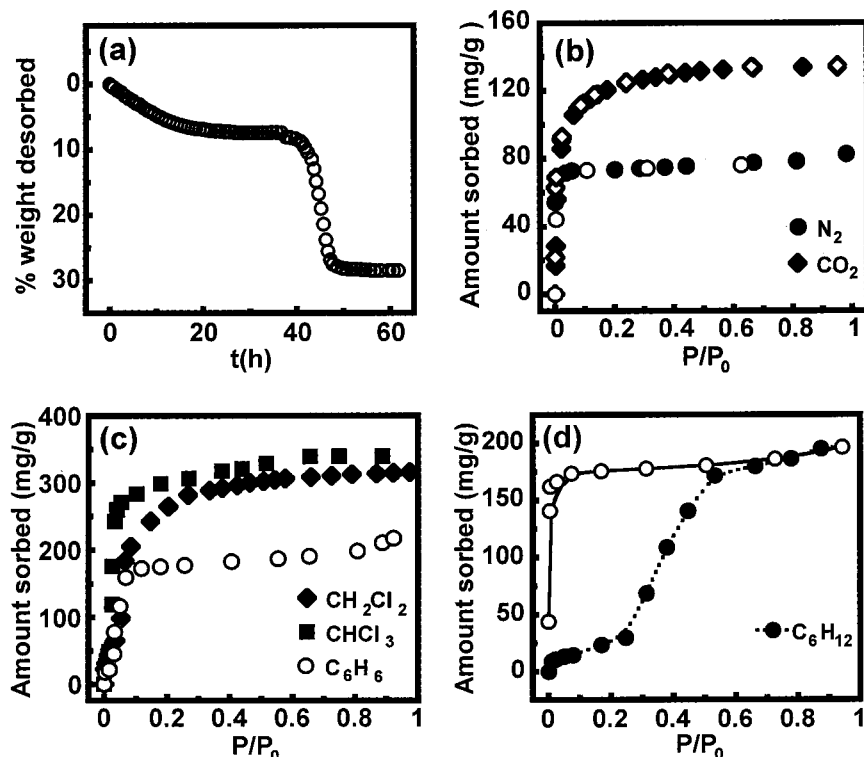


Figure 2. Sorption and desorption data for MOF-2. (a) A plot showing the weight loss due to evacuation of the water ligands and DMF guests. (b–d) Sorption isotherms performed on the evacuated solid (open circles and diamonds in (b) and (d) indicate desorption).

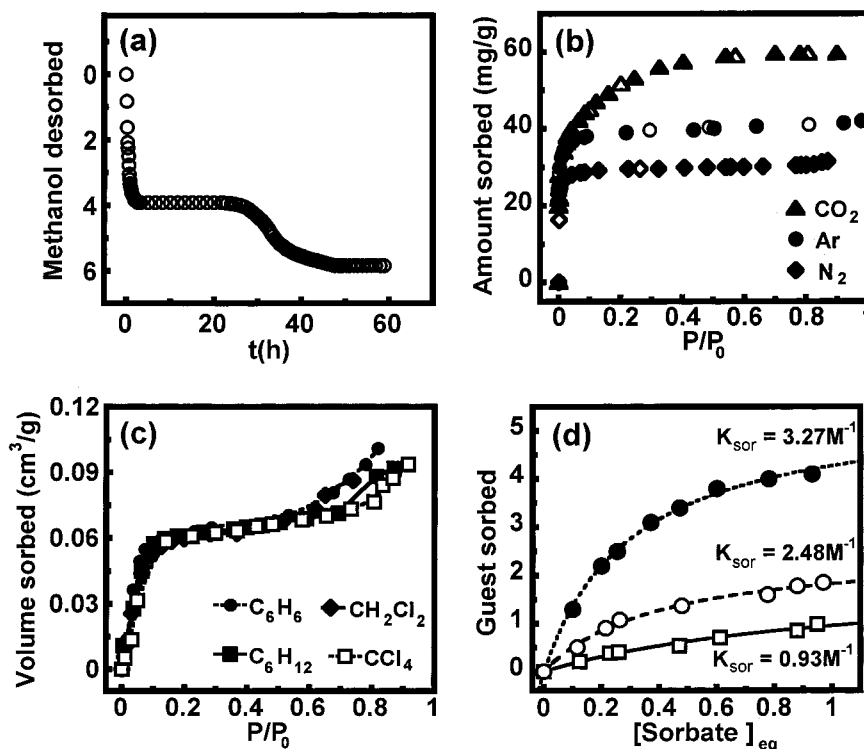


Figure 3. Sorption and desorption data for MOF-3. (a) A plot showing the weight loss due to evacuation of guest and methanol ligand. (b) and (c) Sorption isotherms performed on the evacuated solid (open circles and triangles in b indicate desorption). (d) Liquid sorption isotherms for methanol (filled circles), ethanol (open circles), and *n*-propanol (open squares).

The pore volume derived for MOF-2 from the gas and solvent vapor isotherms (Table 2) has lower values for N_2 and CO_2 perhaps due to their inability to diffuse freely into the pores at low temperature—a complication that is avoided in the case of solvents where the isotherms are measured at room-temperature. A similar trend has been observed for MOF-3 (vide infra). These

cases are in agreement with similar findings documented for zeolite sorption, which are attributed to possible obstruction within the channels that are amplified at lower temperatures.¹⁰

(10) Breck, D. W. *Zeolite Molecular Sieves*; John Wiley & Sons: New York, 1974.

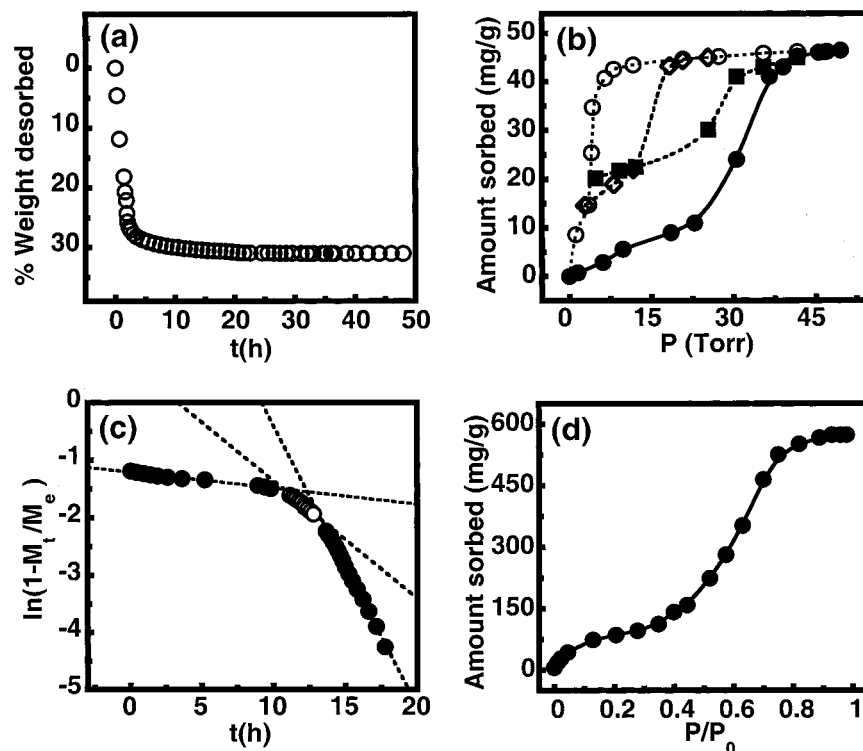


Figure 4. Sorption and desorption data for MOF-4. (a) A plot showing the weight loss due to evacuation of guest and ligand ethanol. (b) Ethanol sorption isotherms at 22 °C (filled circles and open diamonds) and 32 °C (filled squares) with desorption at 22 °C (open circles). (c) Ethanol kinetic sorption at constant pressure plotted as $\ln(1 - M_t/M_e)$ vs time to show the rate constants due to transitions in zinc coordination. (d) Ethanol sorption for the completely evacuated MOF-4 at 22 °C.

Metal–Organic Frameworks with Functionalized Pores.

Unlike MOF-2, the SBUs of MOF-3 and 4, respectively, have methanol and ethanol bound to Zn as terminal ligands. When the SBUs are polymerized using BDC (MOF-3) and BTC (MOF-4), extended porous structures are obtained where the terminal ligands are pointing into the pore space. Removal of the ligands from the framework yields coordinatively unsaturated or accessible zinc centers that ultimately influence the selectivity of the channels for incoming guests.

MOF-3. The trinuclear SBU is extended by BDC into a 3-D network with poly trigonal prismatic topology (Figure 1).^{6f} The central zinc atom is octahedrally bound to carboxylate oxygens, and each of the other zinc centers is coordinated to three such oxygens in addition to two oxygens from terminal methanol ligands, where one methanol is bound more weakly to zinc than the other. In the crystal, two additional methanol molecules are hydrogen bonded to the methanol ligands, thus acting as guests to fill a 3-D channel system of 8 Å cross-section.

Methanol guests can be evacuated at room-temperature, while the ligands can be removed by heating to 140 °C as shown in Figure 3a. The first loss of 14.44% is equivalent to the loss of four methanol guests per formula unit (calcd: 14.54%), while the second loss is equivalent to the removal of two methanol ligands. The overall weight loss (found: 21.53%) is equivalent to the evacuation of five methanol molecules per formula unit (calcd: 21.80%).

Having lost all the methanol implies that the pores within the evacuated framework are functionalized with coordinatively unsaturated zinc centers. Thus, we embarked on a gas and liquid sorption study to show that the framework remains open in the absence of methanol. Here, we found that both the gas and solvent vapor sorption isotherms are of type I behavior as shown in Figure 3b and c, respectively, which clearly indicate that incoming guests can move freely into the channels and the

framework maintains its rigidity and porosity throughout the process. The second increase in sorption as the saturation pressure is approached (Figure 3c) is attributed to sorption on the external crystallite surface. It is worth noting that each of the solvents examined occupy the same crystal free volume as measured at the plateau region ($P/P_0 = 0.5$), lending further support to the reproducible nature of the sorption isotherm measurements and the structural stability of the framework, as well as the presence of homogeneous pores.

In a liquid sorption experiment performed on the partially evacuated derivative, $Zn_3(BDC)_3 \cdot 2CH_3OH$, we found that it does not allow any of the organic solvents examined above into the channels. However, alcohols were permitted, with the expected four methanol guests per formula unit absorbed into the pores (Figure 3d). In fact, the association constant for the sorption of a series of alcohols: methanol, ethanol, and propanol, decreases according to their respective size. We believe that the sorption in this case may be driven by hydrogen bonding interactions between incoming alcohols and the methanol molecules present in the channels, which most likely are bound to zinc. Needless to say, that this is in agreement with the hydrogen bonding pattern found between the methanol guests and ligands in the original crystal structure.

MOF-4. A 3-D porous framework having a 3-D porous system of 14 Å cross-section is produced by polymerizing the dinuclear SBU using BTC as a linker (Figure 1). Here, nitrate counterion is bound to one zinc, while three ethanol molecules are bound as terminal ligands, with the remaining ethanol molecules and water filling the channels.

At room-temperature, 31.2% weight loss is observed, which is equivalent to the loss of four ethanol and one water per formula unit (calcd: 32.0%) (Figure 4a). Heating this material to 72 °C results in a total weight loss of 37.7%, equivalent to the loss of five ethanol and one water (calcd: 38.0%) as shown

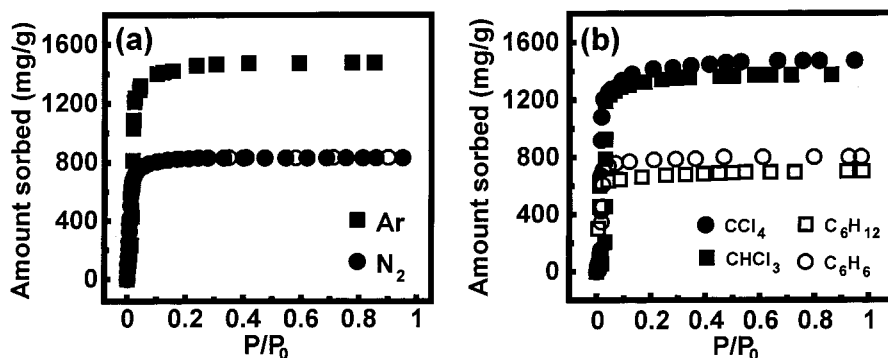


Figure 5. Sorption isotherms for MOF-5. (open circles in (a) indicate desorption).

in Figure 4a. Attempts to measure N_2 , Ar, and CO_2 isotherms of the partially and the fully evacuated forms of this material were unsuccessful, however, it was possible to measure their ethanol vapor sorption isotherm as shown in Figure 4b for the partially evacuated derivative, $Zn_2(BTC)(NO_3) \cdot (C_2H_5OH)$. This has allowed us to achieve a rare glimpse into the local pore environment of MOF-4.

Initially, sorption of ethanol was measured at 22 °C and showed a type V isotherm with large hysteresis (Figure 4b). An initial low uptake was followed by enhanced uptake of ethanol near condensation pressure (~ 30 Torr); reaching a plateau near saturation pressure (~ 46.7 Torr). Two possible reasons can be proposed to account for the initial low uptake. First, as zinc is already in a preferred geometry (tetrahedral), coordination of an additional ethanol is relatively unfavorable, thus producing weakly interacting sorbate and consequently low uptake. Second, in case of pore aperture constriction, it is expected to yield the same isotherm behavior.

To further understand the sorption process at *low pressure*, we examined the isotherm at 32 °C and found slightly higher uptake relative to 22 °C, thus confirming the presence of pore constriction. However, at higher pressure (> 30 Torr) the affect of temperature on sorption is reversed giving higher sorption at 22 °C. This clearly suggests the usual pore filling mechanism for ethanol uptake above 30 Torr, which resumes after all zinc coordination sites have been fully occupied to produce the octahedral geometry found in the original crystal structure. The sorption at the inflection point (30 Torr) of the isotherm is equivalent to nearly three ethanol molecules (acting as ligands to zinc) per formula unit—serving as confirmation of the suggested sorption mechanism.

In another experiment performed on the same sample, we attempted to evacuate only the ethanol guests without removing the ethanol ligands from the pores, then study the resorption of ethanol. The results are presented in Figure 4b, and they are in agreement with the pore filling pattern as a function of temperature. Additionally, as in the case of sorption, the amount resorbed prior to pore filling is equivalent to nearly three ethanol molecules per formula unit, which lends further support to the proposed sorption mechanism.

These findings lead us to conclude that the sorption of ethanol involves an activation process, then coordination to zinc followed by pore filling. Accordingly, the desorption of ethanol shows large hysteresis with a type I desorption pattern, due to the fact that coordinated ethanol ligands are shielded by ethanol guests.

To probe the coordination geometry changes of zinc during the sorption process, we have monitored the weight change with time at constant pressure (46 Torr) and temperature (22 °C) as shown in Figure 4c. These data showed that sorption is

accomplished by three distinct steps having three different rate constants (k): 0.4×10^{-4} , 3.0×10^{-3} , and $8.0 \times 10^{-3} s^{-1}$, which we believe, respectively correspond to the transition from 4- to 5- and 5- to 6-coordination, with the last step representing pore filling.

Ethanol sorption isotherm for the fully evacuated material ($Zn_2(BTC)(NO_3)$) was also measured as shown in Figure 4d. The initial high uptake (0–13 Torr) indicates a strong sorbate-sorbant interaction as evidenced by the shape of the isotherm in that pressure range. This may correspond to the transition of 3-coordinate (unsaturated zinc center) to 4-coordinate zinc. Indeed the amount sorbed in this step is equivalent to one ethanol per formula unit. Thus suggesting the presence of accessible zinc sites, which have sufficient lability toward binding incoming guests.

A Metal–Organic Framework with Unusual Stability and Porosity. Using the rigid tetranuclear supertetrahedral SBU (Figure 1) with BDC yields MOF-5.^{6h} Its structure is derived from a simple cubic 6-connected net in two stages: (a) the nodes (vertices) of the net are replaced by cluster SBUs, and (b) the links (edges) of the net are replaced by finite rods of BDC atoms. The framework atoms in MOF-5 take up only a small fraction of the available space in the crystal, in that, when overlapping spheres with van der Waals radii are placed at the atomic positions, the space not so occupied is 80% of the crystal volume. The pores are a 3-D channel system of 8 Å aperture and 12 Å cross-section. Assuming the same molar volume as in the respective liquids we find that in the original material the guest molecules, $8 \times (8 \text{ DMF} + 1 \text{ C}_6\text{H}_5\text{Cl})$, have a volume of 9512 \AA^3 , which is 55% of the unit cell volume. Indeed, liquid vapor and gas sorption studies indicate (see below) that at 55–61% of the crystal space is accessible to guest species.

Due to their high mobility, the guests in the original as synthesized MOF-5 can be fully exchanged with chloroform. Then the chloroform guests can be easily evacuated from the pores without loss of framework periodicity. In fact, the desolvated single crystals were checked by elemental microanalysis, ^{13}C NMR, mass spectrometry, and thermal gravimetry to confirm the absence of any guests, while optical microscopy was used to show that they have maintained their transparency, morphology, and crystallinity. This has allowed us to perform another X-ray single crystal diffraction study on the fully desolvated form of this framework—a study that revealed mono-crystallinity with cell parameters and atomic positions coincident with those of the as-synthesized material.^{6h} In fact, the highest peaks and lowest valleys in the ΔF map are 0.25 and -0.17 e/\AA^3 scattered randomly both near the framework and the void space. These contrasts with the relatively large values (1.56 and -0.45 e/\AA^3) found in the as-synthesized crystals.

Further evidence for the striking stability of the framework was obtained by heating the fully desolvated crystals in air at 300 °C for 24 h, which had no impact on either their morphology or crystallinity as evidenced by another X-ray single-crystal diffraction study.^{6h} Here, again the cell parameters obtained were unaltered relative to those found for the unheated desolvated crystals. This brings forward unprecedented and unequivocal evidence of framework rigidity and stability in the absence of guest molecules.

The gas and vapor sorption isotherms for the desolvated sample are shown in Figure 5a and b, which are type I and show no hysteresis upon desorption of gases from the pores. Pore volume of 0.61 cm³/cm³ (832 mg/g) was calculated from N₂ sorption—a value unprecedented in the zeolite literature: zeolites which generally have higher molar mass than MOF-5 have pore volumes ranging from 0.18 cm³/cm³ for analcime to 0.47 cm³/cm³ for zeolite A.

Summary

This study demonstrates that multidentate linkers such as BDC and BTC when copolymerized with zinc(II) allow for the formation of rigid metal carboxylate clusters, which act as SBUs in the resulting extended porous network. The inherent structural rigidity of SBUs allow for the formation of stable porous metal–organic solids and their functionalization with accessible metal sites. Specifically, type I isotherms, typical of those obtained

for zeolites and related molecular sieves, are observed for porous metal–organic frameworks as demonstrated for MOF-2, MOF-3, and MOF-5. However, when metal coordinative unsaturation is present in the channels, a more complex sorption processes can occur as observed for ethanol inclusion in MOF-4, where open metal sites largely dictate the sorption mechanism.

Metal–organic frameworks that are robust and have pore volumes exceeding that of zeolites can be achieved by judicious choice of target SBUs as illustrated for MOF-5, which remains in mono-crystalline form even when heated to elevated temperatures in air. Current work is focused on exploiting accessible metal sites for catalysis and sensor applications, and on using the robust frameworks in gas storage and liquid separation technologies. Extension of this work to include more expanded linkers and other metal ions is already in progress.

Acknowledgment. This work is supported by the National Science Foundation (DMR-9980469) and Department of Energy (Division of Chemical Sciences, Office of Basic Energy Sciences, Grant DE-FG03-98ER14903) (O.M.Y.). This effort is part of an ongoing collaboration with Professor M. O’Keeffe (Arizona State University) who acknowledges support by NSF (DMR 9804817).

JA9933386